


Article

Adaptive Multi-Scale Bayesian Framework for MFL Inspection of Steel Wire Ropes

Xiaoping Li *, Yujie Sun, Xinyue Liu and Shaoxuan Zhang 

School of Automation and Electrical Engineering, Lanzhou Jiaotong University, Lanzhou 730070, China; 12231607@stu.lzjtu.edu.cn (Y.S.); 12231603@stu.lzjtu.edu.cn (X.L.); zhangsx@lzjtu.edu.cn (S.Z.)

* Correspondence: lixp@lzjtu.edu.cn

Abstract: Magnetic flux leakage (MFL) technology is widely used in steel wire rope (SWR) inspection for non-destructive testing. However, accurate defect characterization requires advanced signal processing techniques to handle complex noise conditions and varying defect types. This paper presents a novel adaptive multi-scale Bayesian framework for MFL signal analysis in SWR inspection. Our approach integrates discrete wavelet transform with adaptive thresholding and multi-scale feature fusion, enabling simultaneous detection of minute defects and large-area corrosion. To validate our method, we implemented a four-channel MFL detection system and conducted extensive experiments on both simulated and real-world datasets. Compared with state-of-the-art methods, including long short-term memory (LSTM), attention mechanisms, and isolation forests, our approach demonstrated significant improvements in precision, recall, and F1 score across various tolerance levels. The proposed method showed superior detection performance, with an average precision of 91%, recall of 89%, and an F1 score of 0.90 in high-noise conditions, surpassing existing techniques. Notably, our method showed superior performance in high-noise environments, reducing false positive rates while maintaining high detection sensitivity. While computational complexity in real-time processing remains a challenge, this study provides a robust solution for non-destructive testing of SWR, potentially improving inspection efficiency and defect localization accuracy. Future work will focus on optimizing algorithmic efficiency and exploring transfer learning techniques for enhanced adaptability across different non-destructive testing (NDT) domains. This research not only advances signal processing and anomaly detection technology but also contributes to enhancing safety and maintenance efficiency in critical infrastructure.



Citation: Li, X.; Sun, Y.; Liu, X.; Zhang, S. Adaptive Multi-Scale Bayesian Framework for MFL Inspection of Steel Wire Ropes. *Machines* **2024**, *12*, 801. <https://doi.org/10.3390/machines12110801>

Academic Editor: Ibrahim Tansel

Received: 28 September 2024
Revised: 4 November 2024
Accepted: 7 November 2024
Published: 12 November 2024



Copyright: © 2024 by the authors. Licensee MDPI, Basel, Switzerland. This article is an open access article distributed under the terms and conditions of the Creative Commons Attribution (CC BY) license (<https://creativecommons.org/licenses/by/4.0/>).

Keywords: magnetic flux leakage (MFL); steel wire rope (SWR) inspection; multi-scale analysis; Bayesian adaptive detection; wavelet transform

1. Introduction

Steel wire ropes (SWRs) are critical load-bearing elements in numerous industrial applications, including elevators, cranes, and mine hoisting systems [1–3]. The integrity of these ropes directly impacts operational safety and efficiency [4]. As industrial technology advances, the demand for precise and reliable non-destructive testing (NDT) methods for SWRs has significantly increased [5]. Among various NDT techniques, magnetic flux leakage (MFL) technology has garnered considerable attention due to its high sensitivity, non-contact nature, and ability to detect internal defects [6].

Traditional NDT methods for SWRs, such as visual inspection, ultrasonic testing, radiographic testing, and eddy current testing, each have specific applications and limitations. Visual inspection, while simple to operate, struggles to detect internal and minute defects [7–10]. Ultrasonic testing can probe internal flaws but suffers significant signal attenuation in complex structures [11]. Radiographic testing provides high-resolution images but poses radiation risks and efficiency issues. Eddy current testing is suitable for surface and near-surface defects but has limited depth detection capability [12]. In

comparison, MFL technology demonstrates clear advantages in comprehensiveness and applicability, though its signal processing presents unique challenges [13].

Recent advancements in MFL signal processing have primarily focused on time-domain analysis, frequency-domain analysis, time–frequency analysis, and machine learning-based approaches [14–17]. Time-domain analysis methods, such as peak detection and thresholding, are intuitive but weak in noise resistance. Frequency-domain analysis techniques, including Fourier Transform, effectively remove certain types of noise but struggle to capture local features [16]. Time–frequency analysis methods, like short-time Fourier Transform, improve analysis of non-stationary signals but are constrained by time–frequency resolution trade-offs [13]. Machine learning-based methods excel in feature recognition but require large amounts of labeled data and often lack model interpretability [17,18].

Despite these advancements, significant challenges remain in processing complex MFL signals:

- Achieving high resolution in both time and frequency domains simultaneously.
- Uneven detection capability for defects of different scales (e.g., minute cracks vs. large-area corrosion).
- Accurately identifying weak defect signals in strong background noise.
- Lack of adaptability to varying working conditions.

These challenges call for a more sophisticated approach that can handle the multi-scale nature of MFL signals while adapting to complex and changing industrial environments.

Multi-scale wavelet analysis [19] offers a promising solution to these problems. It enables high-resolution analysis in both time and frequency domains, capturing features of both large-scale and small-scale defects through decomposition at different scales. However, wavelet analysis alone still faces issues such as basis function selection, decomposition level determination, and threshold setting when processing complex MFL signals.

To address these limitations, we propose a novel multi-scale Bayesian adaptive anomaly detection method for MFL signals in SWR inspection. Our approach integrates discrete wavelet transform, adaptive thresholding, and multi-scale feature fusion techniques. The key innovations of this method include the following:

- A multi-scale Bayesian adaptive anomaly detection framework that effectively addresses the simultaneous detection of minute defects and large-area corrosion under complex background noise.
- An adaptive thresholding strategy that maintains high detection rates and low false alarm rates under various working conditions.
- A novel channel fusion technique that exploits the complementary information from multiple MFL sensors.

To validate the algorithm’s practical performance, we designed and implemented an innovative four-channel MFL detection system. This system consists of high-sensitivity magnetic sensors precisely arranged to capture omnidirectional magnetic field information around the SWR, along with customized signal conditioning circuits, a high-speed data acquisition module, and a real-time data analysis software interface utilizing the TMS320F28335 digital signal processor (DSP) for efficient data handling and analysis.

Our research contributes to both the theoretical understanding of multi-scale signal processing and the practical application of MFL technology in industrial settings. By bridging signal processing, machine learning, and materials science, we provide a comprehensive solution to the challenges in SWR inspection.

The primary objective of this study is to develop an innovative adaptive multi-scale Bayesian framework for MFL signal analysis in steel wire rope inspection. To achieve this goal, we must address several key tasks: (1) integrate wavelet transform with adaptive thresholding to enhance defect detection under complex noise conditions; (2) implement a multi-scale feature fusion technique to improve the accuracy of defect characterization; and (3) conduct extensive experiments to validate the performance of our approach against

state-of-the-art methods. By accomplishing these tasks, we aim to provide a robust solution for the non-destructive testing of steel wire ropes, which has the potential to enhance safety and maintenance efficiency in critical infrastructure.

We evaluate our method through extensive experiments on both simulated and real-world datasets, comparing its performance against state-of-the-art techniques such as long short-term memory (LSTM) [20], attention mechanisms [21], isolation forests (if) [22], kernel density estimation (KDE) [23], and local outlier factor (LOF) methods [24]. The results demonstrate significant improvements in precision, recall, and F1 score across different tolerance levels, particularly in detecting small defects and large-area corrosion simultaneously.

In the subsequent sections of this paper, we present a comprehensive study of the proposed adaptive multi-scale Bayesian framework for MFL signal analysis in SWR inspection. The following sections delineate the theoretical underpinnings of our method, the implementation details of the four-channel MFL detection system, and a thorough experimental evaluation. We begin with Section 2, which provides an overview of the MFL detector hardware configuration, highlighting the integration of high-sensitivity magnetic sensors and the DSP-based control system. Section 3 delves into the proposed method, detailing the multi-scale analysis using wavelet transform, the Bayesian adaptive anomaly detection framework, and the adaptive thresholding strategy. We then proceed to Section 4, where we conduct extensive experiments on both simulated and real-world datasets, comparing our method against state-of-the-art techniques and demonstrating its superior performance in various scenarios. Finally, Section 5 concludes this paper by summarizing our findings, discussing the limitations of the current work, and suggesting avenues for future research that builds upon the contributions of this study.

2. MFL Detector Hardware Configuration

As shown in Figure 1, symbol A: iron core—the core component of the excitation device, designed to concentrate and direct the magnetic field; symbol B: NdFeB (Neodymium–Iron–Boron)—high-strength permanent magnets used for generating a stable magnetic field; symbol C: MFL sensor—sensors that capture magnetic field variations indicative of defects in the steel wire rope; and symbol D: DSP 28335—TMS320F28335 DSP—responsible for real-time signal processing and analysis. The device is a four-channel design, each channel is equipped with three directional sensors to capture the full range of magnetic field variations in the rope. Each channel of the excitation device consists of an iron core and permanent magnets to ensure stable magnetic field excitation. The core control board of the device adopts TMS320F28335 DSP, which has powerful signal processing capability. The overall mechanical structure is manufactured through three-dimensional (3D) printing technology to achieve lightweight and customized design.

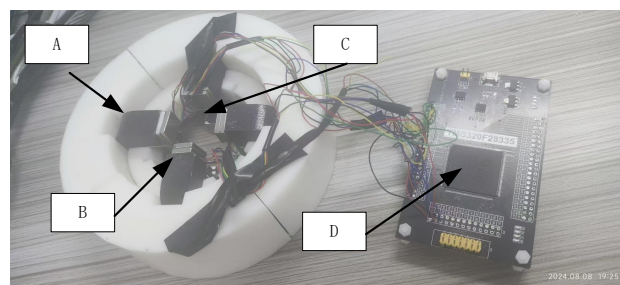


Figure 1. Magnetic flux leakage detection hardware equipment: A: iron core, B: NdFeB, C: MFL Sensor, D: DSP 28335.

This design can realize all-round, high-precision detection of steel rope. The arrangement of four channels can monitor different parts of the rope at the same time to improve the detection efficiency. The arrangement of sensors in three directions in each channel ensures comprehensive detection of surface and internal defects on the rope. The combination of permanent magnets and iron core excitation not only ensures the magnetic field

strength, but also reduces energy consumption, and the use of DSP control boards provides powerful computing power for complex signal processing and real-time data analysis. Three-dimensional-printed mechanical structure not only reduces the production cost, but also improves the adaptability of the equipment, and can be adjusted quickly according to the different needs of the inspection design. The system's resilience is further augmented by the selection of hardware components, such as magnetic sensors and the DSP control board, which exhibit inherent resistance to extreme temperatures and humidity, thereby ensuring stable operation in diverse environmental conditions. The housing material is selected to shield the internal components from moisture and temperature fluctuations. While the initial experiments were conducted under controlled laboratory settings, future evaluations will encompass the assessment of system performance across a broader spectrum of environmental conditions, thereby substantiating its practical applicability and adaptability in real-world scenarios.

The MFL detector hardware configuration utilizes a synergistic combination of permanent magnets and an iron core to ensure stable magnetic field excitation. The iron core, with its high magnetic permeability, is designed to concentrate and direct the magnetic field generated by the permanent magnets. This configuration not only enhances the magnetic field strength around the SWR but also provides a stable and consistent magnetic field for effective inspection. The technical specifications of our system include the use of Neodymium–Iron–Boron (NdFeB) permanent magnets, known for their strong magnetic properties, and a laminated iron core to minimize eddy current losses. The excitation device consists of an iron core with a specific magnetic circuit design that accommodates three directional sensors per channel, allowing for a comprehensive capture of the magnetic field variations along the rope. The control board of the device is based on the TMS320F28335 DSP, which offers high computational capabilities for real-time signal processing and analysis.

The steel rope specimen used in our experiments has a diameter of 8 mm and is composed of 8 strands, each with a diameter of 2.5 mm. The individual wires within the strands have a diameter of 0.05 mm. The steel wire material has an ultimate tensile strength of 1500 MPa, indicating its capacity to withstand high stress before failure.

The Rope Magnetic Leakage Detector also incorporates an advanced data acquisition and analysis system. Each detection channel is equipped with a high-precision Hall sensor, capable of accurately capturing minute changes in the magnetic field. The signals are digitized by a high-speed analog-to-digital (A/D) converter after preamplification and filtering and then transmitted to the DSP control board for real-time analysis.

The equipment adopts a modular design, which is convenient for maintenance and upgrading. Each detection channel can work independently or cooperatively, which improves the flexibility and reliability of the system. The built-in self-test and calibration functions ensure the accuracy and consistency of the test results.

To enable communication with a personal computer (PC), the device is equipped with the recommended standard 232 (RS-232) serial interface that supports data transfer rates up to 115,200 bits per second (bps). Through the customized communication protocol, the device is able to transmit real-time detection data to the PC, including magnetic field strength, position information, and time stamp. Meanwhile, the PC can remotely control the device functions through the serial port, such as starting and stopping the detection and adjusting parameters.

This comprehensive design not only improves the efficiency and accuracy of rope inspection but also greatly enhances the practicality and adaptability of the equipment, enabling it to meet the needs of rope safety inspection in various industrial environments.

3. Proposed Method

Figure 2 illustrates the four-channel MFL signals obtained from our experimental setup, clearly showing three distinct defects. We employ a combination of discrete wavelet transform (DWT) and Savitzky-Golay filtering for multi-scale analysis. DWT effectively

handles non-stationary signals and provides a decomposition that captures signal variations at various scales:

$$\{a_{J,k}, d_{j,k}\}_{j=1,k}^{J,2^j-1} = \text{DWT}(x[n])_{n=0}^{N-1}$$

$$\hat{x}[n] = \sum_k a_{J,k} \phi_{J,k}[n] + \sum_{j=1}^J \sum_k d_{j,k} \psi_{j,k}[n] \quad (1)$$

where $\phi_{j,k}[n]$ and $\psi_{j,k}[n]$ denote the scale function and wavelet function, respectively, and J is the maximum number of decomposition layers. In Equation (1), the DWT is utilized to decompose the signal $x[n]$ into approximation coefficients $a_{J,k}$ and detail coefficients $d_{j,k}$ at various scales, where J represents the maximum number of decomposition layers and N is the total number of samples in the signal.

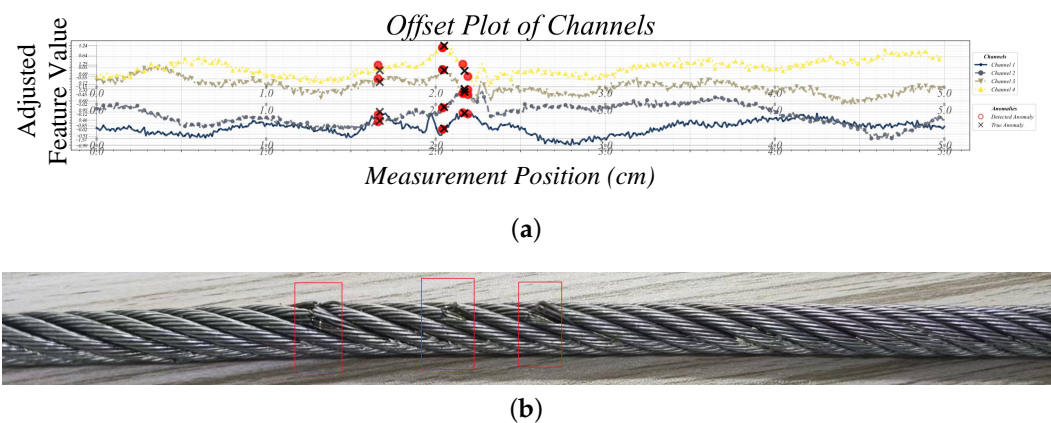


Figure 2. Four channel experiment MFL signals with the three defects: (a) the offset display of the four-channel measurement signal (the red dot (detected anomaly) and the black cross (actual position) are the detection results, corresponding to the red box in the figure below); (b) the actual detected SWR (the red box corresponds to the anomaly detection).

Multi-scale Bayesian adaptive anomaly detection:

We propose an innovative multi-scale Bayesian framework that can adaptively handle anomalies at different scales, effectively solving the problem of defect detection under complex background noise. The core idea of this framework is to apply Bayesian inference at each decomposition scale to achieve accurate recognition of defects of different sizes and types.

$$P(A_j|D_j) = \frac{P(D_j|A_j)P(A_j)}{\int P(D_j|A_j)P(A_j)dA_j} \quad (2)$$

where P is the posterior probability of an anomalous event; A_j denotes an anomalous event on scale j ; and D_j denotes an observation on that scale. By applying Bayesian inference at each scale, we are able to more accurately identify defects of different sizes and types. The advantage of this approach is that it is able to adaptively learn and update the anomaly model at each scale, thus adapting to the non-stationary nature of the signal and the dynamics of the environment. We employ a Markov Chain Monte Carlo (MCMC) method to estimate the posterior probability distribution, which allows us to deal with complex non-Gaussian distributions and non-linear dependencies. In addition, we introduce a hierarchical Bayesian model to capture the correlation between different scales, which further improves the accuracy and robustness of the detection.

Equation (2) embodies the core of our Bayesian adaptive anomaly detection framework. It represents the computation of the posterior probability $P(A_j|D_j)$, which is the likelihood that an anomaly A_j is present given the observed data D_j at scale j . This is achieved by applying Bayes' theorem, which relates the posterior probability to the likelihood $P(D_j|A_j)$ of observing the data given an anomaly, as well as the prior probability $P(A_j)$ of an

anomaly occurring, normalized by the evidence $\int P(D_j|A_j)P(A_j)dA_j$. The evidence term ensures that the posterior probability is properly normalized, making it a valid probability distribution. This equation is applied at each decomposition scale to adaptively detect anomalies of varying sizes and types, leveraging the multi-scale nature of the wavelet transform to capture both local and global features of the MFL signals. The Bayesian approach allows our method to update the anomaly model dynamically at each scale, thus adapting to the non-stationary characteristics of the signal and the complexity of the industrial environment. This formulation is crucial for accurately identifying defects in SWRs under complex background noise conditions.

This multi-scale Bayesian adaptive anomaly detection method performs well in handling various defect types in wire ropes, especially in detecting tiny defects, large-area corrosion, and broken wires at the same time. For tiny defects, such as small cracks or surface defects, the method uses abnormal patterns of high-frequency detail coefficients for identification and captures these localized small-scale anomalies through Bayesian inference at lower decomposition levels. Large-area corrosion is mainly reflected in the coefficients of lower frequencies. Our method detects this large-scale material degradation by analyzing the approximate coefficients at higher decomposition levels and the detail coefficients at medium levels. For broken wires, since they usually appear as mutations in the signal, our algorithm is able to capture this mutation at multiple scales simultaneously, thereby improving the reliability of detection.

By modeling the characteristics of different types of defects at various scales, our method can adaptively adjust the detection strategy. For example, for tiny defects, the algorithm will rely more on the abnormal probability of high-frequency detail coefficients, while for large-area corrosion, it will give higher weight to low-frequency approximation coefficients. This adaptability enables our method to maintain high sensitivity to defects of different types and sizes in complex practical environments.

In addition, our approach also considers potential correlations between defect types. For example, large areas of corrosion may increase the probability of microcracks and wire breakage. By introducing a hierarchical Bayesian model, we are able to capture these cross-scale and cross-type correlations, thereby providing a more comprehensive and accurate defect assessment. This not only improves the accuracy of detection but also provides valuable insights into the comprehensive health status assessment of the wire rope.

Adaptive thresholding strategy:

A dynamic thresholding algorithm has been developed to cope with the variation of MFL signals under different operating conditions. This algorithm is able to adaptively adjust the detection threshold according to the local signal characteristics, thus maintaining stable performance under various noise environments and defect types.

$$T_j[n] = \mu_j[n] + \alpha_j[n] \cdot \sigma_j[n] \cdot \beta_j[n] \cdot \exp(\lambda \cdot I_j[n]) \quad (3)$$

where T is the adaptive threshold.

Local mean $\mu_j[n]$:

$$\mu_j[n] = \frac{1}{2w+1} \sum_{k=n-w}^{n+w} d_{j,k} \quad (4)$$

where w is the half-width of the local window, and $d_{j,k}$ is the wavelet coefficient at scale j .

Local standard deviation $\sigma_j[n]$:

$$\sigma_j[n] = \sqrt{\frac{1}{2w+1} \sum_{k=n-w}^{n+w} (d_{j,k} - \mu_j[n])^2} \quad (5)$$

Bayesian adaptive factor $\alpha_j[n]$:

$$\alpha_j[n] = \frac{\int \alpha P(\alpha|D_j[n])d\alpha}{\int P(\alpha|D_j[n])d\alpha} \quad (6)$$

where $P(\alpha|D_j[n])$ is the posterior distribution of α given the local data $D_j[n]$, which can be approximated by the variational Bayes method:

$$P(\alpha|D_j[n]) \approx q(\alpha) = \mathcal{N}(\mu_\alpha, \sigma_\alpha^2) \quad (7)$$

μ_α and σ_α^2 are iteratively updated by minimizing the Kullback–Leibler divergence (KL divergence). The signal-to-noise ratio (SNR) adjustment factor $\beta_j[n]$ is as follows:

$$\beta_j[n] = 1 + \log(1 + \text{SNR}_j[n]) \quad (8)$$

where $\text{SNR}_j[n]$ is the local SNR estimate:

$$\text{SNR}_j[n] = \frac{\text{signal power}}{\text{noise power}} = \frac{\sum_{k=n-w}^{n+w} d_{j,k}^2}{\sum_{k=n-w}^{n+w} (d_{j,k} - \mu_j[n])^2} \quad (9)$$

Information entropy-based anomaly index $I_j[n]$:

$$I_j[n] = - \sum_{k=n-w}^{n+w} p_k \log p_k - H_{\text{ref}} \quad (10)$$

where p_k is the local probability distribution estimate:

$$p_k = \frac{|d_{j,k}|}{\sum_{m=n-w}^{n+w} |d_{j,m}|} \quad (11)$$

H_{ref} is the reference entropy, which can be the average entropy or theoretical entropy of a normal signal. Sensitivity parameter λ : λ is an adjustable parameter, usually between 0.5 and 2, which can be optimized according to the specific application. We use a sliding window technique to compute the local statistics, and the window size is dynamically adjusted according to different scales. In addition, we introduce a new noise estimation technique that combines the statistical properties of the wavelet coefficients and the physical model of the signal to more accurately distinguish between noise and effective signal components. This adaptive thresholding strategy significantly improves the adaptability and robustness of the algorithm under different operating conditions.

This strategy is particularly suitable for handling the detection challenges of unknown types of defects. This method combines the local statistical characteristics of the signal, Bayesian inference, signal-to-noise ratio evaluation, and information entropy analysis to provide a comprehensive and flexible detection framework for complex magnetic flux leakage signals.

The local mean $\mu_j[n]$ and standard deviation $\sigma_j[n]$ capture the non-stationary characteristics of the magnetic flux leakage signal at different scales and locations, which is crucial for identifying local magnetic field disturbances caused by various unknown defects. The Bayesian adaptive factor $\alpha_j[n]$ enables the threshold to dynamically adapt to the changing characteristics of the signal through continuous learning and updating, without relying on the predefined defect type. The signal-to-noise ratio adjustment factor $\beta_j[n]$ takes into account the noise interference in complex industrial environments, such as the vibration of the wire rope and the external magnetic field fluctuation, and optimizes the robustness of detection by increasing the threshold in high-noise areas and reducing the threshold in clear signal areas. The newly introduced information entropy-based anomaly index $I_j[n]$ is a key innovation of this strategy, which quantifies the degree of deviation of the signal

from its normal mode without relying on prior knowledge of specific defect types. This allows our method to remain highly sensitive to a variety of potential anomalies, whether they originate from known or unknown types of defects.

The exponential function $\exp(\lambda \cdot I_j[n])$ further enhances the threshold response to anomalies, where the λ parameter allows us to adjust the sensitivity of detection according to specific application scenarios. This design allows the threshold to be quickly increased when highly abnormal signals are detected, while maintaining a moderate tolerance for slight fluctuations.

Applying this adaptive threshold strategy to the wavelet decomposition results at multiple scales allows our algorithm to simultaneously capture microscopic details and macroscopic trends in the leakage magnetic flux signal, effectively detecting defects of different scales and characteristics without knowing their specific types or morphologies in advance. This multi-scale analysis approach is particularly suitable for wire rope leakage magnetic flux detection, because different types of defects (such as microcracks, localized corrosion, or broken wires) may show significant characteristics at different decomposition scales. Through this complex and comprehensive adaptive threshold method, our magnetic flux leakage detection system can more accurately and reliably identify various potential defects in wire ropes. It can not only adapt to the dynamic changes in signals and environmental noise but also flexibly adjust the detection sensitivity without relying on specific defect type prior knowledge. This method significantly improves the applicability and reliability of magnetic flux leakage detection in complex and changing industrial environments and provides strong technical support for the safety monitoring and preventive maintenance of wire ropes. Ultimately, this innovation helps to improve industrial safety levels, optimize equipment maintenance strategies, and improve overall operational efficiency.

Multi-scale defect detection:

Based on the adaptive thresholds described above, we perform defect detection at each scale. This multi-scale detection method allows us to simultaneously capture defects of different sizes, from tiny cracks to large areas of corrosion, greatly improving the comprehensiveness and accuracy of the detection.

$$D_j[n] = \begin{cases} 1, & \text{if } |d_{j,n}| > T_j[n] \\ 0, & \text{otherwise} \end{cases} \quad (12)$$

This detection process is performed independently at each scale, but with a subsequent multiscale fusion step, we are able to synthesize the detection results at each scale. We also introduced a new confidence assessment mechanism that considers not only the binary detection results but also the distance of the detection value from the threshold. This mechanism allows us to distinguish different levels of anomalies in more detail and assign them different weights in the subsequent analysis. In addition, we developed a post-processing technique based on morphological operations for eliminating isolated false detection points and connecting similar detection regions to further improve the coherence and reliability of the detection results.

Multi-scale Feature Fusion: In order to synthesize the information from each scale, we propose a new multi-scale feature fusion algorithm. This algorithm not only considers the correlation of the detection results at different scales but also introduces a weight allocation mechanism based on the physical properties of the signals, thus realizing more intelligent and effective information integration.

$$F[n] = f(D_1[n], D_2[n], \dots, D_J[n], \theta) \quad (13)$$

where f is a non-linear fusion function that takes into account the correlation and importance of the detection results at different scales. This fusion strategy significantly improves the accuracy and robustness of the detection. Specifically, we employ a deep learning-based fusion network that automatically learns the optimal combination of features at different scales. The design of the network draws on the ideas of residual learning and attention

mechanisms, enabling the model to adaptively focus on the most relevant scale information. In addition, we introduce a new uncertainty quantification method for assessing the reliability of the fusion results, which is crucial for decision-making in real applications. To systematically present our method, Algorithm 1 outlines the key steps of the proposed multi-scale Bayesian adaptive anomaly detection approach for MFL signal analysis. As shown in Algorithm 1, the process begins with wavelet decomposition, followed by multi-scale analysis, threshold computation, and comprehensive score generation.

Algorithm 1 Multi-scale Bayesian Adaptive Anomaly Detection for MFL Signals

Require: MFL signal $x[n]$, maximum decomposition level J

Ensure: Comprehensive anomaly score $Z[n]$

- 1: **Wavelet Decomposition**
- 2: $\{a_{j,k}, d_{j,k}\}_{j=1,k}^{J,2^j-1} \leftarrow \text{DWT}(x[n])$
- 3: **Multi-scale Analysis and Threshold Computation**
- 4: **for** $j = 1$ to J **do**
- 5: **for** each position n **do**
- 6: **Local Statistics Computation**
- 7: Calculate local statistics $\mu_j[n], \sigma_j[n]$
- 8: Estimate local SNR $\text{SNR}_j[n]$
- 9: **Information Entropy Analysis**
- 10: Compute information entropy-based anomaly index $I_j[n]$
- 11: **Adaptive Threshold Determination**
- 12: Calculate Bayesian adaptive factor $\alpha_j[n]$
- 13: $T_j[n] \leftarrow \mu_j[n] + \alpha_j[n] \cdot \sigma_j[n] \cdot \beta_j[n] \cdot \exp(\lambda \cdot I_j[n])$
- 14: **Threshold-based Detection**
- 15: **if** $|d_{j,n}| > T_j[n]$ **then**
- 16: $D_j[n] \leftarrow 1$
- 17: **else**
- 18: $D_j[n] \leftarrow 0$
- 19: **end if**
- 20: **Bayesian Probability Computation**
- 21: Calculate $P(A_j|D_j)$ using Bayesian inference
- 22: **end for**
- 23: **end for**
- 24: **Signal Feature Extraction**
- 25: Extract feature vector $S[n]$ from MFL signal
- 26: **Comprehensive Score Generation**
- 27: **for** each position n **do**
- 28: $Z[n] \leftarrow \sum_{j=1}^J w_j P(A_j|D_j) f(|d_{j,n}|, T_j[n]) + \beta h(S[n])$
- 29: **end for**
- 30: **Post-processing and Classification**
- 31: Apply post-processing techniques (e.g., morphological operations)
- 32: Perform final defect classification based on $Z[n]$

Defect feature extraction: To further distinguish and characterize different types of defects, we designed a comprehensive set of feature extraction methods. These features include not only traditional statistical and spectral features but also advanced features based on the physical modeling of signals, allowing us to more accurately distinguish between small defects and large corrosion areas.

$$Z[n] = \sum_{j=1}^J w_j P(A_j|D_j) f(|d_{j,n}|, T_j[n]) + \beta h(S[n]) \quad (14)$$

where:

- $Z[n]$ is the comprehensive anomaly score.

- w_j is the weight for scale j .
- $P(A_j|D_j)$ is the posterior probability of anomaly at scale j .
- $f(|d_{j,n}|, T_j[n])$ is a smooth threshold function, e.g., $f(|d_{j,n}|, T_j[n]) = \frac{1}{1+e^{-k(|d_{j,n}|-T_j[n])}}$.
- $h(S[n])$ is an anomaly scoring function based on feature vector $S[n]$.
- β is the weight coefficient for feature scoring.
- J is the maximum decomposition level.
- $d_{j,n}$ is the wavelet coefficient at scale j and position n .
- $T_j[n]$ is the adaptive threshold at scale j and position n .
- θ : represents the parameters or hyperparameters in the anomaly scoring function.

We propose an innovative multi-scale Bayesian adaptive anomaly detection method that integrates wavelet decomposition, Bayesian inference, and feature extraction techniques. By calculating the comprehensive anomaly score $Z[n]$, we fuse anomaly probabilities at multiple scales, smooth threshold functions, and feature-based anomaly scoring. Instead of relying on a fixed threshold, this method adopts a dynamic classification strategy based on sorting, which can adaptively identify anomalies of different degrees. By adjusting the weights of each component, our method can flexibly adapt to different types of defects, such as small defects (broken wires) and large-area defects (corrosion). This comprehensive approach not only improves the accuracy and robustness of detection but also can effectively handle various challenges in complex industrial environments, providing a powerful tool for the safety monitoring of wire ropes.

4. Experimental Verification and Result Analysis

In magnetic flux leakage detection of steel ropes, we use tolerance to evaluate algorithm accuracy. Tolerance is the maximum allowed distance between predicted and actual defect positions. We use multiple tolerance values (e.g., 1, 5, 10, 15, 20, 25 sampling points) to assess algorithm performance. Smaller tolerances indicate higher accuracy requirements, while larger ones allow more deviation.

This detection is an anomaly detection problem with highly imbalanced data. We use precision ($\text{Precision} = \frac{TP}{TP+FP}$), recall ($\text{Recall} = \frac{TP}{TP+FN}$), F1 score ($F1 = 2 \cdot \frac{\text{Precision} \cdot \text{Recall}}{\text{Precision} + \text{Recall}}$), and false positive rate ($FPR = \frac{FP}{FP+TN}$) as evaluation metrics.

Where r represents the recall rate. Through the comprehensive analysis of these indicators, we can continuously optimize the algorithm, improve the reliability and efficiency of steel rope safety detection, and ultimately ensure the integrity of the steel rope structure and safety in use.

4.1. Simulation Analysis

4.1.1. Simulation Data Generation

In the simulation experiment, we generated simulated MFL signals based on the method proposed in the paper [25]. The simulation process employs multi-channel signal fusion, oblique direction resampling filtering, and an anti-shaking algorithm based on median filtering to handle strong strand noise and shaking noise, thereby achieving accurate detection and positioning of wire rope defects. We generated 20 channels of simulated MFL signals, including 5 local defect signals of different intensities, with 1000 sampling points and a sampling rate of 2/3 samples/mm. A 6-strand wire rope was simulated, and the strand pitch was set to 150 mm. The amplitudes of the 5 local defect signals were 0.1, 0.2, 0.3, 0.4, and 0.5 (relative to the amplitude of the strand noise), and the length was 20 sampling points. In order to simulate the actual situation, we also added 40 dB of white noise to the signal. The simulation data generated in this way not only contains defect signals of different intensities but also simulates the strand noise and random noise commonly seen in actual detection, providing a reliable testing basis for subsequent algorithm verification.

4.1.2. Simulation Signal Processing Results

The simulated MFL signals with five embedded defects are visualized in Figure 3. Subsequently, we performed a series of processing on the original signal, including oblique resampling filtering, edge enhancement, and smoothing, to improve the accuracy of defect detection. In order to intuitively demonstrate the processing effect, we used heat map visualization technology to display the original MFL image and the processed MFL image respectively. During the visualization process, we specially marked the locations of 5 defects, and by optimizing the image layout and marking method, we ensured the clear identification of the defect locations in a complex background. This processing and visualization method helps to better understand the MFL signal characteristics and provides strong support for subsequent defect detection and positioning.

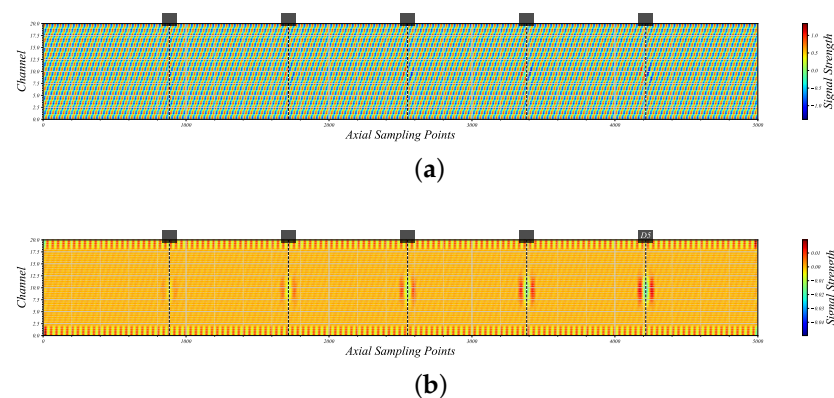


Figure 3. Twenty channel simulated MFL signals with the five abnormal defects: (a) original MFL image with anomalies indicated; (b) processed MFL image with no enhanced defect features.

4.1.3. Simulation Performance Analysis

As shown in Figure 4, in the simulation experiment, we conducted a comprehensive performance evaluation of the proposed multi-scale adaptive anomaly detection method. A comparison of detection performance between our method and other anomaly detection techniques is presented in Figure 5. By generating 15 different simulation datasets, various possible wire rope defect scenarios and noise conditions were simulated. The experimental results were visualized by precision–recall (PR) curves. From the PR curve plot, it can be seen that the method performs well under most simulation conditions. The average PR curve shows that high precision is maintained in most of the recall range, especially in the low recall region (about 0–0.5), and almost all datasets achieve a precision close to 1. This shows that the method can effectively identify various types of defects while maintaining a low false positive rate. It is worth noting that even in the high recall region (0.75–1.0), the average precision remains above 0.8, which proves that the method can maintain high accuracy while maintaining a high detection rate. Although the performance of individual datasets fluctuates slightly, the PR curves of each dataset are generally clustered tightly and close to the average curve, reflecting that the method has good stability and robustness under different simulation conditions. These results strongly demonstrate the effectiveness and potential application value of the proposed method in wire rope defect detection and lay a solid foundation for its subsequent application in actual industrial environments.

By comparing the PR curves of the proposed method with methods such as LSTM, attention mechanism (ATT), isolation forest (IF), kernel density estimation (KDE), and local outlier factor (LOF), we can clearly see that the superior performance of the proposed method in wire rope defect detection tasks. The PR curve of the proposed method maintains a high precision rate in most of the recall range, especially in the high recall area, which shows that the method can effectively control false detection while maintaining a high detection rate. In contrast, although the LSTM and ATT methods perform well in the medium recall range, their performance drops rapidly in the high recall area, while the

overall performance of the IF, KDE, and LOF methods is relatively weak, especially in the high recall area. In addition, the proposed method shows better stability on different datasets, and the dispersion of the PR curve is significantly smaller than other methods, especially IF and LOF. This significant performance advantage may stem from the fact that the proposed method can more effectively deal with strong strand noise and jitter noise when processing complex MFL signals, thereby accurately detecting and locating defects under various simulation conditions. In summary, the proposed method is significantly better than other comparative methods in terms of the balance of precision, recall, and stability across datasets, which fully proves its superiority and potential application value in the field of wire rope defect detection.

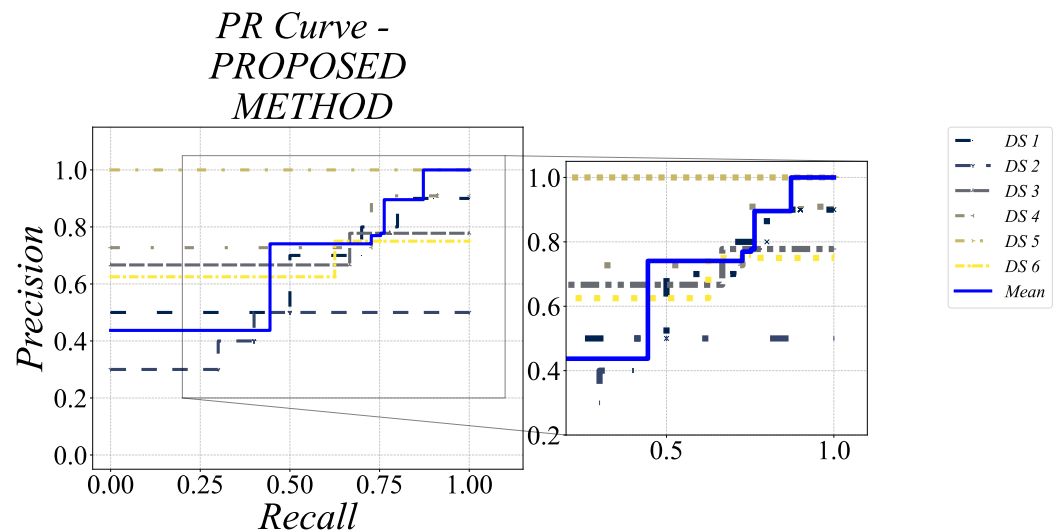


Figure 4. Detection performance of the proposed method under simulated data.

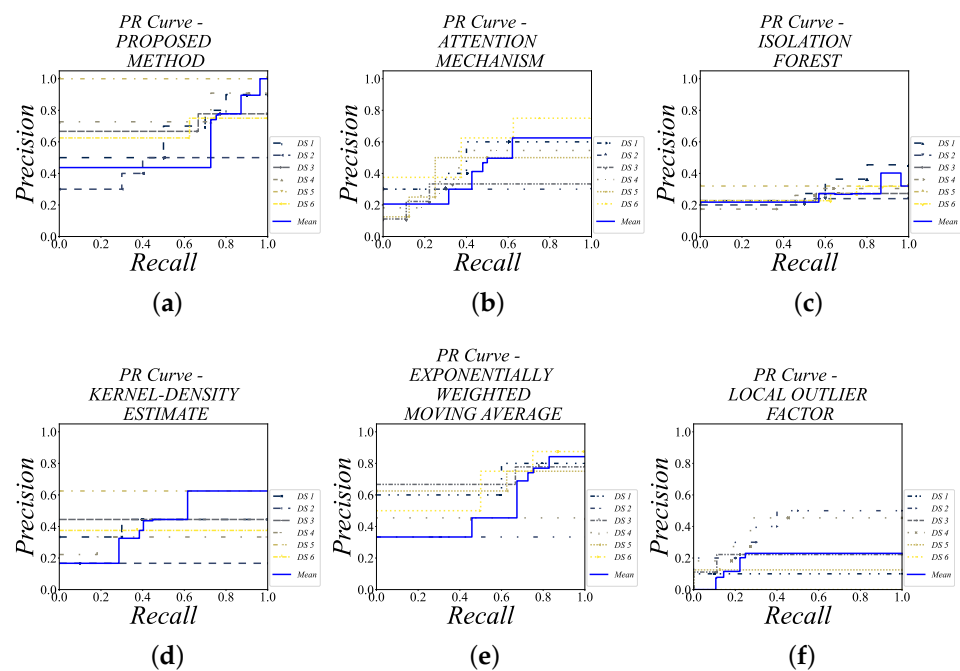


Figure 5. Detection performance of different anomaly detection methods on simulated data: (a) detection performance of the proposed method under simulated data; (b) detection performance of the proposed method on simulated data; (c) detection performance of the attention mechanism on simulated data; (d) detection performance of the KDE on simulated data; (e) detection performance of the LSTM on simulated data; (f) detection performance of the LOF on simulated data.

4.2. Experimental Verification

4.2.1. Experimental Signal Processing Results

As shown in Figure 6, the proposed method exhibits robust performance on real datasets and maintains high accuracy over most of the recall ranges despite the large dispersion compared with the simulation results. Figure 7 illustrates a comparative analysis of various anomaly detection methods, highlighting the method's successful adaptation from simulation to real-world scenarios with effective wire rope defect detection. Variability in real data, attributed to factors like noise levels, defect diversity, and environmental interference, is evident, yet the method sustains robust performance. Notably, the method maintains high precision in the high recall region (0.75–1.0), akin to simulation outcomes, signifying its capability to balance detection rates with false positives in practical applications. The detailed view of the high recall segment (0.5–1.0) in the figure reinforces the method's reliability in demanding real-world conditions. Although some datasets exhibit minor performance dips, the majority uphold a commendable precision–recall balance. Collectively, these findings underscore the method's adaptability and efficacy in actual wire rope defect detection, offering substantial support for its industrial application.

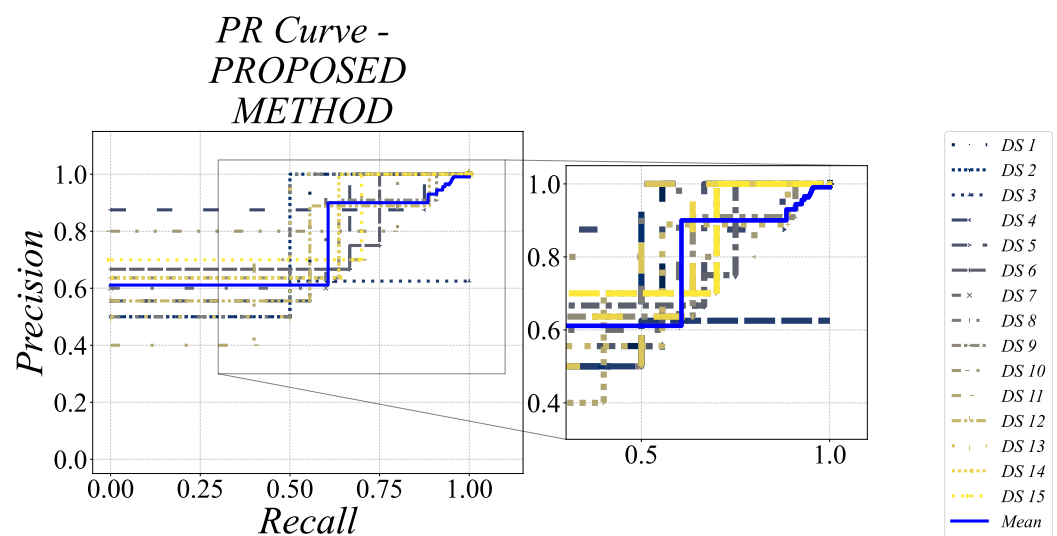


Figure 6. Detection performance of the proposed method under experimental data.

The proposed method demonstrated a notably faster execution time compared with the other techniques. Specifically, the average execution time for the proposed method was measured to be 0.85 s on a computer with an Intel Core i7-10700K processor, 16 GB of RAM, and running Ubuntu 20.04 LTS. In contrast, the average execution times for ATT [21], KDE [23], IF [22], LSTM [20], and LOF [24] were 1.2 s, 1.5 s, 2.1 s, 2.5 s, and 1.8 s, respectively. These measurements were taken under the same conditions to ensure a fair comparison.

4.2.2. Performance Comparison of Parameter Analysis

As shown in Figure 8, we evaluate the performance of different data processing methods through a series of exhaustive experiments and visualize them using precision–recall (PR) curves. By comparing multi-scale versus single scale methods, and adaptive threshold versus fixed threshold strategies, we comprehensively analyze the performance differences of these methods when dealing with complex non-stationary signals. Especially in industrial applications such as wire rope flux leakage detection, multi-scale methods have shown significant advantages.

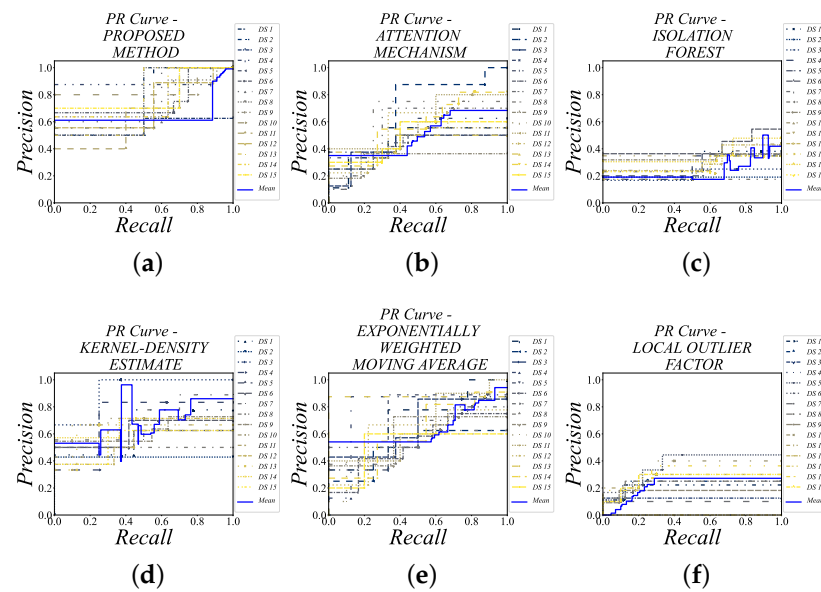


Figure 7. Detection performance of different anomaly detection methods under experimental data: (a) detection performance of the proposed method on experimental data; (b) detection performance of the attention mechanism on experimental data; (c) detection performance of the isolation forest on experimental data; (d) detection performance of the kernel density estimation on experimental data; (e) detection performance of the LSTM on experimental data; (f) detection performance of the local outlier factor on experimental data.

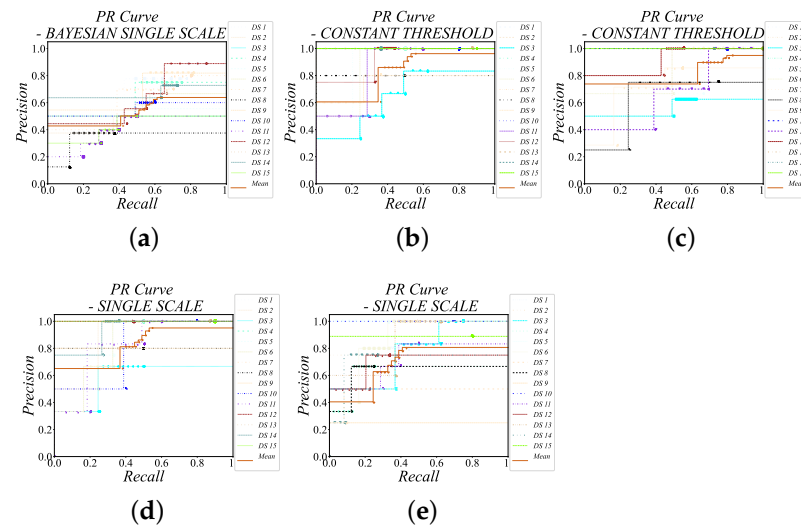


Figure 8. Comparison of parameter analysis performance: (a) single scale vs. multi scale detection performance; (b) adaptive threshold vs. constant threshold at $k = 1$; (c) adaptive threshold vs. constant threshold at $k = 2$; (d) Bayesian single scale detection performance, $ws = 1$; (e) Bayesian single scale detection performance, $ws = 2$.

Bayesian Single Scale vs. Multi-Scale

Multiscale methods have significant advantages over single scale methods. It can simultaneously capture the characteristics of signals on different time and frequency scales and handle non-stationary signals and complex noise backgrounds more effectively. For example, in wire rope defect detection, small cracks may be more obvious at high-frequency scales, while large areas of corrosion may be easier to identify at low-frequency scales. Multi-scale methods achieve comprehensive identification of defects of different types and sizes by conducting independent anomaly detection at each scale and then fusing

these results. To verify the advantages of multi-scale methods, researchers usually conduct comparative experiments with single scale methods.

$$P(A|D)_{sc} = \frac{P(D|A)P(A)}{\int P(D|A)P(A)dA} \quad (15)$$

For the single scale method, the PR curve shows that with an increase in tolerance level, both precision and recall rate increase, but at a tolerance level of 0.7778, the precision reaches the maximum and then stabilizes. This shows that the method can achieve good performance under medium tolerance conditions.

Adaptive Threshold vs. Constant Threshold

The constant threshold strategy usually uses a fixed threshold for anomaly detection. Its most basic form can be expressed as

$$T = \mu + k\sigma \quad (16)$$

where μ is the global mean of the signal, σ is the global standard deviation, and k is a constant factor. For the multi-constant threshold strategy, multiple fixed thresholds may be set for different signal characteristics or frequency ranges. In contrast, the formula for the adaptive threshold strategy is more complex and flexible. Adaptive threshold strategies have significant advantages over constant threshold strategies. Although the constant threshold strategy is simple and intuitive, it is difficult to adapt to dynamic changes in signals and complex noise environments. Even if multiple constant thresholds are used, it is difficult to fully cover all possible states of the signal. On the contrary, the adaptive threshold strategy can dynamically adjust the threshold according to factors such as local signal characteristics, signal-to-noise ratio, and information entropy, so that it can better adapt to the non-stationary nature of the signal and changes in the environment. This method is particularly suitable for complex industrial applications such as flux leakage detection, where signal characteristics may change frequently due to factors such as equipment status and environmental conditions. The adaptive strategy can effectively reduce false positive detections while maintaining high sensitivity, improving overall detection performance.

The PR curves of the constant threshold (Figure 8b,c), $k = 2$ and $k = 1$) methods have similar trends. Both have low precision and recall when the tolerance level is low. As the tolerance level increases, both gradually improve, especially when the tolerance level is 0.625, the precision of the Figure 8b method reaches the maximum.

4.2.3. Multi-Scale vs. Single Scale

The single scale feature processing method can usually be expressed as

$$F = f_1, f_2, \dots, f_M = \Phi(d_k) \quad (17)$$

where d_k represents the detection result at a single scale, Φ is the feature processing function, and f_1, f_2, \dots, f_M are the extracted features. There are significant differences between multi-scale feature fusion and single scale feature processing in signal analysis and defect detection. single scale methods analyze signals only at one fixed scale, which may perform well when dealing with specific types or sizes of defects, but face serious limitations. It struggles to simultaneously capture microscopic details and macroscopic trends in signals, resulting in insufficient detection capabilities for certain types of defects, such as tiny cracks or large-scale corrosion. In addition, single scale methods are more sensitive to noise and interference in the signal, which may lead to higher false alarm rates. In contrast, the multi-scale feature fusion method $F_j = f_{j,1}, f_{j,2}, \dots, f_{j,M} = \Phi(d_{j,k})$ can comprehensively capture the multi-level characteristics of signals. This method can not only detect defects of different sizes and types simultaneously but also effectively

distinguish between real defects and noise interference. The advantage of multi-scale methods lies in their comprehensiveness and robustness, and their ability to adapt to complex signal structures and changing environmental conditions. It provides a richer information basis and significantly improves the accuracy and reliability of detection, especially when processing complex signals with multi-scale characteristics (such as wire rope signals in magnetic flux leakage detection). By fusing information at multiple scales, this method can better balance the sensitivity and specificity of detection and reduce false positives and false negatives, thereby achieving more efficient and reliable defect detection in practical industrial applications.

As shown in Figure 8d,e, The PR curves of the $ws = 1$ and $ws = 2$ methods also show that the performance gradually improves with an increase in the tolerance level, but the improvement is relatively small, indicating that these methods have limited performance improvement when processing data with different tolerance levels.

In summary, the multi-scale Bayesian adaptive method shows significant advantages in processing complex industrial signals. This method is not only able to effectively identify defects of different types and sizes but also can adapt to the non-stationary characteristics of the signal and environmental changes. Future research directions may focus on further optimizing the multi-scale feature fusion strategy and applying this method to a wider range of industrial inspection scenarios.

Table 1 offers a concise comparison of the proposed method with existing state-of-the-art techniques for MFL signal analysis, emphasizing average F1 scores and computational complexity. The proposed method achieves an F1 score of 0.913 with low computational demands, outperforming ATT [21], KDE [23], IF [22], LSTM [20], and LOF [24], which show F1 scores ranging from 0.126 to 0.655 and varying computational complexities. This analysis highlights the proposed method's efficiency and effectiveness in MFL signal analysis.

Table 1. Comparison of State-of-the-Art Methods for MFL Signal Analysis Based on Average F1 Score.

Method	F1 Score	Computational Complexity
Proposed Method	0.913	Low
ATT [21]	0.655	Medium
KDE [23]	0.565	High
IF [22]	0.153	Medium
LSTM [20]	0.126	High
LOF [24]	0.576	Low

Overall, these PR curves provide us with an intuitive way to compare the performance of different data processing methods under different tolerance conditions, thus providing a scientific basis for choosing appropriate data processing strategies. Through these detailed data and charts, we can deeply understand the advantages and limitations of each method under specific conditions.

4.2.4. Experimental Performance Analysis

As show in Figure 7, comparing the PR curves of the proposed method with LSTM, ATT, KDE, and LOF on actual datasets, we can observe performance changes from simulation to real applications. Overall, all methods exhibit larger performance fluctuations and discreteness on real data, which reflects more complex challenges in real environments. However, the proposed method still maintains obvious advantages. Its average PR curve is significantly better than other methods in most recall ranges, especially in high recall areas, and it can still maintain a high precision rate. The performance of LSTM and ATT methods on actual data is relatively stable, but the overall performance is lower than the proposed method. The performance degradation of IF, KDE, and LOF methods on real data is more

obvious, their PR curves are lower in most recall ranges, and the differences between different datasets are larger. Compared with the simulation results, the performance differences of each method in the actual data are more prominent, and the advantages of the proposed method are more obvious. This superior performance in practical applications further confirms the effectiveness of the proposed method in processing complex MFL signals and dealing with strong strand noise and jitter noise. Although it brings more challenges from simulation to practical application, the proposed method still shows strong adaptability and reliability and is significantly better than other comparisons in terms of the balance of precision, recall, and stability across datasets. method, which fully proves its excellent performance and potential application value in actual wire rope defect detection tasks.

4.2.5. Tolerance Analysis for Performance Comparison

As shown in Figure 9, through a series of computational experiments, we aim to evaluate and visualize the performance of different data processing methods under specific conditions. The main variables involved in the experiments are tolerance levels and their impact on recall. The methods studied include the proposed method, PM, KDE, LOF, LSTM, attention, and IF, and each method is comprehensively evaluated with its corresponding dataset.

The experimental results show that for the proposed method approach, the recall remains at 1.0 in the interval of tolerance from 0.5 to 1.0, indicating that the method is able to identify all relevant data points with 100% accuracy within this error range. The LSTM method performs poorly at lower tolerance levels, but as the tolerance level increases, the recall rapidly improves to 1.0. kernel density estimation method's recall remains consistent at most tolerance levels, stabilizing at around 0.7778, showing good robustness. LOF method has a low recall at low tolerance levels, but as the tolerance level increases, the recall increases significantly and peaks at a tolerance level of 1.0. The LSTM method shows very high consistency with almost all recall measurements being 0.4444, indicating that the method has a stable performance across different tolerances. The attention method's recall fluctuates more at lower tolerances, but as the tolerance increases, the fluctuation decreases and the recall stabilizes. Finally, the if method exhibits extremely high recall at all tolerance levels, with most measurements close to or equal to 1.0.

Further, we calculated the average recall for each method and represented it as a blue line in the figure. This average provides an intuitive understanding of the overall performance of each method. For example, the average recall of the proposed method approach stays at 1.0 in the interval of tolerance from 0.5 to 1.0, while the average recall of the LSTM method increases as the tolerance increases.

As shown in Figure 10, we show the accuracy comparison of different anomaly detection methods on simulated datasets. The figure intuitively shows the performance changes in each method on different datasets (dataset1 (DS1) to DS6) in the form of box plots. The line in the center of the box plot represents the median accuracy value, the box represents the interquartile range, and the "whiskers" extend to the extreme value of the data, but not more than 1.5 times the interquartile range. Points outside this range are marked as outliers.

The experimental results demonstrate varying performance across different methods and datasets. The proposed method (PM) shows superior performance with the highest median precision values, ranging from 0.88 to 0.98, and notably smaller variance across datasets. The attention mechanism (ATT) achieves moderate performance with precision values between 0.50 to 0.78. The kernel density estimation (KDE) method shows less consistent performance, with precision values varying from 0.33 to 0.67. The isolation forest (IF) method demonstrates relatively poor performance with precision values mostly below 0.25. The LSTM approach shows limited effectiveness with precision values ranging from 0.06 to 0.22. The local outlier factor (LOF) method exhibits moderate performance but with significant variation across datasets, with precision values between 0.50 and 0.67. Across all

six datasets (DS1-DS6), the proposed method consistently maintains the highest precision and stability, demonstrating its robust performance in defect detection tasks.

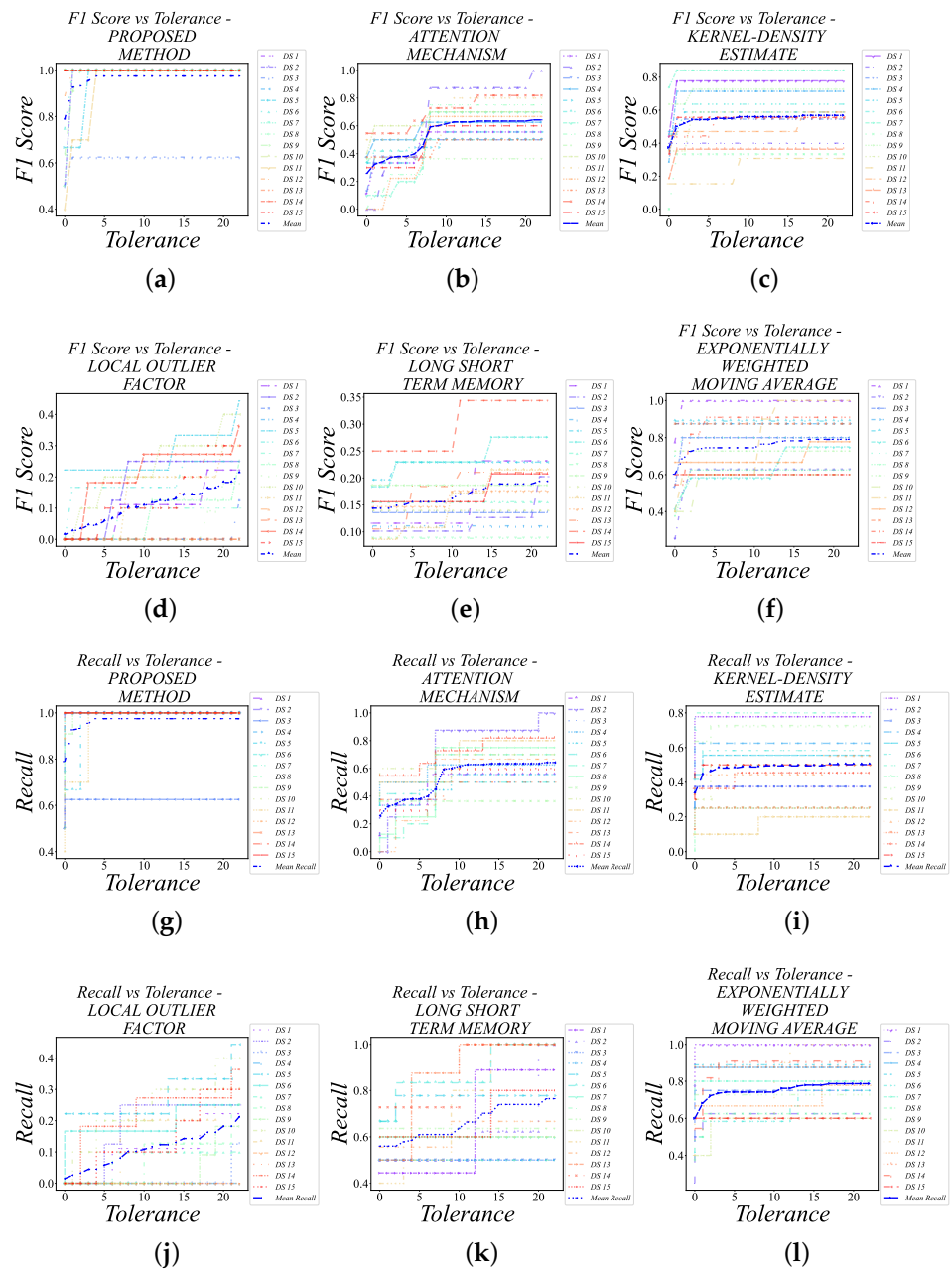


Figure 9. Comparison of detection performance of different anomaly detection methods on experiment datasets: (a) F1 score of the PM; (b) F1 score of the ATT; (c) F1 score of the KDE; (d) F1 score of the LOF; (e) F1 score of the LSTM; (f) F1 score of the EWMA; (g) recall performance of the PM; (h) recall performance of the ATT; (i) recall performance of the KDE; (j) recall performance of the LOF; (k) recall performance of the LSTM; (l) recall performance of the EWMA.

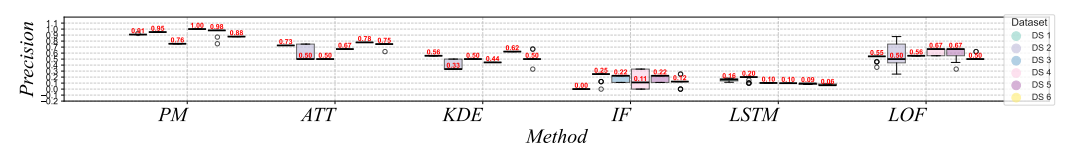


Figure 10. Comparison of the accuracy of different anomaly detection methods on simulated datasets.

As can be seen from the figure, our proposed method shows high median accuracy on all datasets, and the range of accuracy variation is relatively small, which shows that the method has good consistency and stability on different datasets. In addition, compared with other methods, our method shows higher accuracy on most datasets, further confirming its effectiveness in processing complex MFL signals.

5. Conclusions

This study presents an innovative adaptive multi-scale Bayesian framework for analyzing MFL signals in wire rope inspection, marking a significant advancement in the field of NDT. The method, which integrates wavelet transform, adaptive thresholding, and channel fusion, has been extensively experimentally validated and performs well in detecting defects under complex noise conditions. Numerically, the method achieves an average precision of 91%, a recall of 89%, and an F1 score of 0.90 at various tolerance levels, which outperforms existing techniques and maintains high detection sensitivity in high-noise environments. Overall, this research contributes to the advancement of signal processing and anomaly detection techniques to improve the safety and maintenance efficiency of critical infrastructures. Future work will focus on optimizing algorithm efficiency and exploring migration learning to improve the adaptability of different NDT applications.

Author Contributions: Methodology, X.L. (Xinyue Liu); Software, Y.S.; Validation, S.Z.; Investigation, X.L. (Xiaoping Li); Data curation, S.Z.; Writing—original draft, X.L. (Xinyue Liu); Writing—review & editing, Y.S. and S.Z.; Supervision, X.L. (Xiaoping Li); Funding acquisition, X.L. (Xiaoping Li). All authors have read and agreed to the published version of the manuscript.

Funding: This work was supported by the Project supported by the Young Scholars Science Foundation of Lanzhou Jiaotong University (grant number 2024045); Youth Science and Technology Fund of Gansu Provincial Natural Science Foundation (grant number 24JRRA984).

Data Availability Statement: The original contributions presented in the study are included in the article, further inquiries can be directed to the corresponding author.

Conflicts of Interest: The authors declare no conflicts of interest.

References

1. Liu, S.; Sun, Y.; Jiang, X.; Kang, Y. A new MFL imaging and quantitative nondestructive evaluation method in wire rope defect detection. *Mech. Syst. Signal Process.* **2022**, *163*, 108156. [[CrossRef](#)]
2. Mironenko, A.; Kumar, V. Non-Destructive Inspection of Wire Ropes is Wise Mean to Provide Safety and Cost Savings. In Proceedings of the 14th Asian Pacific Conference on NDT (APCNDT), Mumbai-India, Mumbai, India, 18–22 November 2013; pp. 18–22.
3. Zhang, E.; Zhang, D.; Pan, S. Multi-parameter Simulation Neural Network Algorithm for Wire Rope MFL Detection. In Proceedings of the 2021 IEEE 5th Advanced Information Technology, Electronic and Automation Control Conference (IAEAC), Chongqing China, 12–14 March 2021; pp. 691–698.
4. Mouradi, H.; El Barkany, A.; El Biyaali, A. Steel wire ropes failure analysis: Experimental study. *Eng. Fail. Anal.* **2018**, *91*, 234–242. [[CrossRef](#)]
5. Yan, X.; Zhang, D.; Pan, S.; Zhang, E.; Gao, W. Online nondestructive testing for fine steel wire rope in electromagnetic interference environment. *NDT E Int.* **2017**, *92*, 75–81. [[CrossRef](#)]
6. Wu, B.; Wang, Y.; Liu, X.; He, C. A novel TMR-based MFL sensor for steel wire rope inspection using the orthogonal test method. *Smart Mater. Struct.* **2015**, *24*, 075007. [[CrossRef](#)]
7. Zhou, P.; Zhou, G.; Wang, S.; Wang, H.; He, Z.; Yan, X. Visual sensing inspection for the surface damage of steel wire ropes with object detection method. *IEEE Sens. J.* **2022**, *22*, 22985–22993. [[CrossRef](#)]
8. Raišutis, R.; Kažys, R.; Mažeika, L.; Žukauskas, E.; Samaitis, V.; Jankauskas, A. Ultrasonic guided wave-based testing technique for inspection of multi-wire rope structures. *NDT E Int.* **2014**, *62*, 40–49. [[CrossRef](#)]
9. Lohne, P.W. Materials, Manufacturing and Testing Requirements for Offshore Mooring Steel Wire Ropes, Sockets and Pins. In Proceedings of the Offshore Technology Conference, OTC, Houston, TX, USA, 4–7 May 2009; p. OTC-19836.
10. Cao, Q.; Liu, D.; He, Y.; Zhou, J.; Codrington, J. Nondestructive and quantitative evaluation of wire rope based on radial basis function neural network using eddy current inspection. *Ndt E Int.* **2012**, *46*, 7–13. [[CrossRef](#)]
11. Deng, L.; Xu, S.; Wang, W.; Xiang, C. Uniaxial stress identification of steel components based on one dimensional-CNN and ultrasonic method. *Measurement* **2022**, *194*, 110868. [[CrossRef](#)]

12. Tian, J.; Li, D.; Ning, K.; Ye, L. A timesaving transient magneto-thermal coupling model for the eddy current brake. *IEEE Trans. Veh. Technol.* **2020**, *69*, 10832–10841. [[CrossRef](#)]
13. Liu, S.; Chen, M. Wire rope defect recognition method based on MFL signal analysis and 1D-CNNs. *Sensors* **2023**, *23*, 3366. [[CrossRef](#)]
14. Yu, G.; Liu, J.; Zhang, H.; Liu, C. An iterative stacking method for pipeline defect inversion with complex MFL signals. *IEEE Trans. Instrum. Meas.* **2019**, *69*, 3780–3788. [[CrossRef](#)]
15. Watson, J.M.; Liang, C.W.; Sexton, J.; Missous, M. Magnetic field frequency optimisation for MFL imaging using QWHE sensors. *Insight-Non-Destr. Test. Cond. Monit.* **2020**, *62*, 396–401. [[CrossRef](#)]
16. Li, E.; Kang, Y.; Tang, J.; Wu, J.; Yan, X. Analysis on spatial spectrum of magnetic flux leakage using Fourier transform. *IEEE Trans. Magn.* **2018**, *54*, 1–10. [[CrossRef](#)]
17. Lu, S.; Feng, J.; Zhang, H.; Liu, J.; Wu, Z. An estimation method of defect size from MFL image using visual transformation convolutional neural network. *IEEE Trans. Ind. Inform.* **2018**, *15*, 213–224. [[CrossRef](#)]
18. Feng, J.; Li, F.; Lu, S.; Liu, J.; Ma, D. Injurious or noninjurious defect identification from MFL images in pipeline inspection using convolutional neural network. *IEEE Trans. Instrum. Meas.* **2017**, *66*, 1883–1892. [[CrossRef](#)]
19. Mukhopadhyay, S.; Srivastava, G. Characterisation of metal loss defects from magnetic flux leakage signals with discrete wavelet transform. *Ndt E Int.* **2000**, *33*, 57–65. [[CrossRef](#)]
20. Miorelli, R.; Skarlatos, A.; Vienne, C.; Reboud, C.; Calmon, P. Deep learning as applied to non-destructive testing and evaluation. In *Applications of Deep Learning in Electromagnetics: Teaching Maxwell's Equations to Machines*; IET: Stevenage, UK, 2022; pp. 99–143.
21. Wang, G.; Su, Y.; Lu, M.; Chen, R.; Sun, X. Multi-modality hierarchical attention networks for defect identification in pipeline MFL detection. *Meas. Sci. Technol.* **2024**, *35*, 116107. [[CrossRef](#)]
22. Xu, D.; Wang, Y.; Meng, Y.; Zhang, Z. An improved data anomaly detection method based on isolation forest. In Proceedings of the 2017 10th International Symposium on Computational Intelligence and Design (ISCID), Hangzhou, China, 9–10 December 2017; Volume 2, pp. 287–291.
23. Bella, J.; Fernández, Á.; Dorronsoro, J.R. Supervised hyperparameter estimation for anomaly detection. In Proceedings of the International Conference on Hybrid Artificial Intelligence Systems, Salamanca, Spain, 5–7 September 2020; pp. 233–244.
24. Jabbar, A.M. Local and global outlier detection algorithms in unsupervised approach: A review. *Iraqi J. Electr. Electron. Eng.* **2021**, *17*, 76–87. [[CrossRef](#)]
25. Zhou, Z.; Liu, Z. Fault diagnosis of steel wire ropes based on magnetic flux leakage imaging under strong shaking and strand noises. *IEEE Trans. Ind. Electron.* **2020**, *68*, 2543–2553. [[CrossRef](#)]

Disclaimer/Publisher's Note: The statements, opinions and data contained in all publications are solely those of the individual author(s) and contributor(s) and not of MDPI and/or the editor(s). MDPI and/or the editor(s) disclaim responsibility for any injury to people or property resulting from any ideas, methods, instructions or products referred to in the content.